

# Catalytic and Computational Studies of N-Heterocyclic Carbene or Phosphine-Containing Copper(I) Complexes for the Synthesis of 5-Iodo-1,2,3-Triazoles

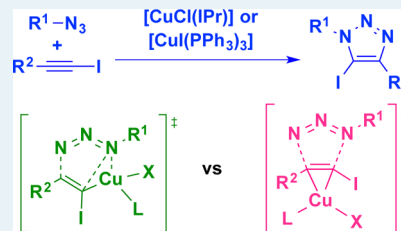
Steven Lal, Henry S. Rzepa, and Silvia Díez-González\*

Department of Chemistry, Imperial College London, Exhibition Road, South Kensington, SW7 2AZ London, United Kingdom

## Supporting Information

**ABSTRACT:** Two complementary catalytic systems are reported for the 1,3-dipolar cycloaddition of azides and iodoalkynes. These are based on two commercially available/readily available copper complexes,  $[\text{CuCl}(\text{IPr})]$  or  $[\text{CuI}(\text{PPh}_3)_3]$ , which are active at low metal loadings ( $\text{PPh}_3$  system) or in the absence of any other additive ( $\text{IPr}$  system). These systems were used for the first reported mechanistic studies on this particular reaction. An experimental/computational-DFT approach allowed to establish that (1) some iodoalkynes might be prone to dehalogenation under copper catalysis conditions and, more importantly, (2) two distinct mechanistic pathways are likely to be competitive with these catalysts, either through a copper(III) metallacycle or via direct  $\pi$ -activation of the starting iodoalkyne.

**KEYWORDS:** azide, iodotriazole, copper, cycloaddition, click chemistry



## INTRODUCTION

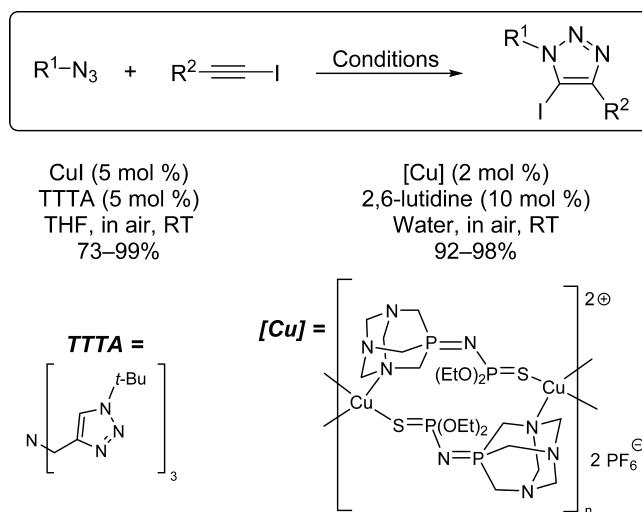
The versatility and value of heterocycles for a wide range of applications feeds the continuous synthetic drive for novel and better methodologies aimed at their preparation. Halogenated heterocycles are of particular interest, because of their easier derivatization, notably via cross-coupling reactions. 1,3-Dipolar cycloadditions, Huisgen reactions,<sup>1</sup> are one of the most general approaches to five-membered heterocycles, and the preparation of 1,2,3-triazoles from organic azides and terminal alkynes in particular (CuAAC) has witnessed a true explosion since the discovery of copper(I) species as outstanding and selective catalysts for this reaction.<sup>2</sup>

Despite the important applications that CuAAC has found in biochemistry, materials, or medicinal science,<sup>3</sup> it remains largely limited to terminal alkynes. This is not surprising if we take into account the well-accepted intermediacy of copper-acetylide derivatives in the formation of 1,2,3-triazoles.<sup>4</sup> Hence, besides two isolated examples,<sup>5</sup> only halogenated alkynes have been shown to be active toward cycloaddition reactions under copper catalysis to date. The first reported example was based on a combination of copper(I) and copper(II) salts for the reaction of azides and bromoalkynes in THF.<sup>6</sup> However, it was not until 2009 that this reaction began attracting the interest of the chemical community, when Fokin and co-workers reported the use of polytriazole as ligands in the preparation of 5-iodotriazoles.<sup>7</sup>

In great contrast with the cycloaddition of terminal alkynes, where the ligandless combination  $\text{CuSO}_4/\text{Na}$  ascorbate is very popular, the presence of coordinating ligands has proved essential for any iodotriazole to be formed. Hence, simple amines such as triethylamine or DIPEA (diisopropylethylamine) were screened by the Fokin group, but it was a tris-

triazole ligand (TTTA) and CuI (5 mol % each) that provided the best yields (Scheme 1). An iminophosphorane-copper(I) complex led to similar results with a lower copper loading of 2 mol % in aqueous media.<sup>8</sup> Here, besides the ancillary ligands, an excess of lutidine with respect to the catalyst was required for the reaction to proceed (Scheme 1). Remarkably, in both cases,

**Scheme 1. Reported Catalysts for the Cycloaddition of Azides and Iodoalkynes**



Received: March 12, 2014

Revised: May 26, 2014

Published: May 29, 2014

filtration or extraction techniques directly yielded analytically pure products.

A third catalytic system, phenylethynylcopper(I) in combination with 2 equiv of  $\text{NEt}_3$ , has also been reported for two specific examples.<sup>9,10</sup> The small number of catalysts known for the synthesis of iodotriazoles is in stark contrast with the impressive array of those reported for the cycloaddition reactions of terminal alkynes. This is a clear indication of the bigger catalytic challenge that the cycloaddition of iodoalkynes represents.

Tris-triazoles, and TTTA in particular, remain the most popular ligands for this reaction,<sup>11</sup> and the only ones that have found application in larger systems, such as the functionalization of polymers<sup>12</sup> and preparation of phthalocyanines.<sup>13</sup> Despite its efficiency, important drawbacks remain for the general use of this family of ligands in this transformation. First of all, contrary to copper salts, tris-triazole compounds are extremely expensive.<sup>14</sup> Alternatively, the preparation of TTTA requires tris-propargylamine, and *t*-butyl azide. The latter compound is particularly hazardous, because of its low molecular weight, which greatly increases the risk of explosion of organic azides.<sup>15</sup> Finally, tris-triazoles are not the best candidates for undertaking mechanistic studies, since Finn and co-workers showed that, because of their relatively weak donor properties, multiple coordination modes to copper centers are possible, depending on the reaction media and cycloaddition partners.<sup>16</sup>

In consequence, the development of safe and more convenient catalysts is fundamental for iodotriazoles to have a real impact, as has been the case for the related 5-H-1,2,3-triazoles.<sup>17</sup> Capitalizing on our experience with copper-mediated cycloaddition reactions,<sup>18</sup> we decided to explore the activity of well-established copper(I) catalysts bearing either phosphine or N-heterocyclic carbene ancillary ligands. Herein, we report the catalytic activity of such complexes in the cycloaddition reaction of organic azides and iodoalkynes, as well as, the mechanistic studies carried out for this transformation.

## RESULTS AND DISCUSSION

**(A). Catalytic Studies. Copper(I) Complexes Bearing N-Heterocyclic Carbene Ligands.** Within the last 20 years, N-heterocyclic carbenes (NHCs) have gained a prominent place in the chemist's toolbox, thanks to their outstanding affinities to metal centers in all oxidation states, which have naturally led to their widespread application in organic synthesis.<sup>19</sup> Copper–NHC complexes are not an exception, and they are recognized to be stable species while remaining effective catalysts for many transformations.<sup>20</sup>

Neutral  $[\text{CuX}(\text{NHC})]$  complexes ( $\text{X} = \text{Cl}, \text{Br}, \text{or I}$ )<sup>18b</sup> were first tested in the model reaction of benzyl azide and iodoethynylbenzene. For the readers' convenience, the NHC ligands used in this study and their acronyms are shown in Figure 1.

For  $[\text{CuX}(\text{NHC})]$  complexes bearing an IAd ligand, the trend in conversion was  $\text{X} = \text{I} > \text{Br} > \text{Cl}$  (see Chart 1). IMes proved to be a better ligand and, contrary to the IAd complexes, a reverse reactivity trend was observed, with  $[\text{CuCl}(\text{IMes})]$  slightly outperforming  $[\text{CuBr}(\text{IMes})]$ . Saturated NHC ligands SIMes and SIPr were also screened with SIMes, leading to a higher conversion of 76% over 24 h. The NHC ligands in Chart 1 are ordered by increasing percent buried volume,<sup>21</sup> and the IPr ligand appears to perfectly meet the

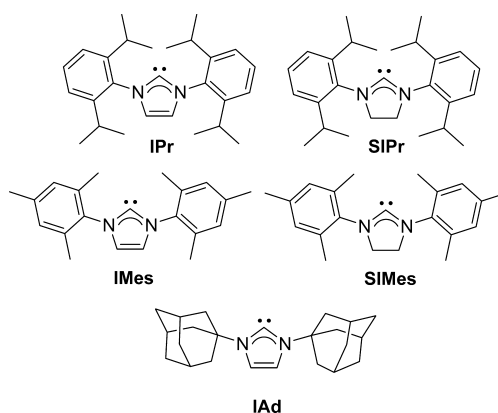
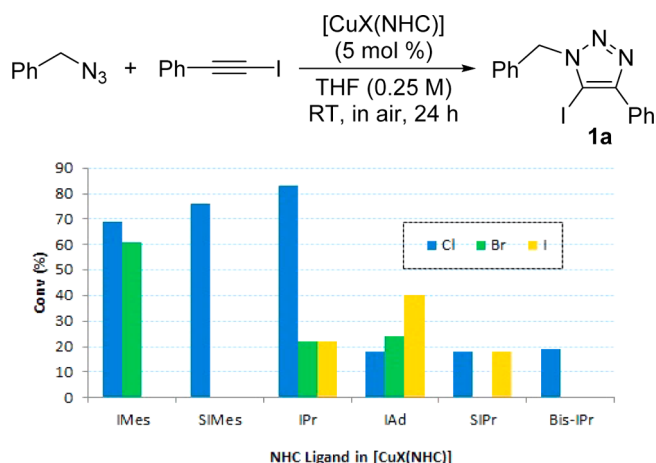


Figure 1. N-Heterocyclic carbene ligands.

### Chart 1. Copper(I)–NHC Catalyst Screening<sup>a</sup>



<sup>a</sup><sup>1</sup>H NMR conversions are the average of at least two independent experiments. Bis-IPr =  $[\text{Cu}(\text{IPr})_2]\text{PF}_6$ .

steric requirements for this particular reaction, as both more or less bulky NHC ligands led to lower conversions to **1a**. Overall, the commercially available  $[\text{CuCl}(\text{IPr})]$  clearly outperformed all of the screened complexes, including its bromide and iodide analogues (Chart 1). For comparison purposes, the related cationic complex  $[\text{Cu}(\text{IPr})_2]\text{PF}_6$ <sup>22</sup> was also tested in the model reaction, but only 19% conversion was observed under otherwise identical reaction conditions.

In all cases, the expected 5-iodotriazole **1a** was formed exclusively, without any trace of the corresponding 5-H-triazole. It is important to note that no correlation could be found when comparing the activity of each of these  $[\text{CuX}(\text{NHC})]$  complexes in this reaction and in the related terminal alkyne–azide cycloaddition.<sup>18b</sup> This might be indicative of significantly dissimilar mechanistic pathways in both transformations.

The most promising catalyst,  $[\text{CuCl}(\text{IPr})]$  was then tested in different solvents. No conversion was observed in DMF, DMSO, 1,4-dioxane, toluene, or MeOH, and only very sluggish reactions took place in MeCN (5%), acetone (5%), or water (17%). Remarkably, the reaction proceeded equally well in THF or in the absence of solvent (83 and 88% conversion, respectively). Surprisingly, in more concentrated reaction mixtures (0.5 or 1 M in THF, compared to 0.25 M) only very poor conversions into triazole **1a** were observed. On the other hand, decreasing the concentration to 0.1 M, also

inhibited the cycloaddition. Thus, either neat conditions or 0.25 M in THF are optimal for the cycloaddition reactions of azides and iodoalkynes in the presence of [CuCl(IPr)].

Considering the crucial importance that nitrogen-based ligand/additives have had in the previously reported systems for this reaction (even with preformed catalysts<sup>9</sup>), we next tested some of them in an attempt to further increase the conversion in the model reaction (Table 1). Triethylamine,

**Table 1.** Effect of Nitrogen-Containing Additives with [CuCl(IPr)]

$\text{Ph-CH}_2\text{-N}_3 + \text{Ph-C}\equiv\text{C-I} \xrightarrow[\text{Neat, in air, RT, 24 h}]{\text{[CuCl(IPr)] (5 mol \%), Additive (5 mol \%)}} \text{Ph-CH}_2\text{-N}_2\text{C(Ph)=C(I)-Ph}$ <p style="text-align: center;"><b>1a</b></p>		
entry	additive	conv (%) <sup>a</sup>
1	none	88
2	NEt <sub>3</sub>	89
3	DIPEA	87
4	2,6-lutidine	81
5 <sup>b</sup>	2,6-lutidine	28
6	1,10-phenanthroline	0
7 <sup>c</sup>	1,10-phenanthroline	0

<sup>a</sup><sup>1</sup>H NMR conversions are the average of at least two independent experiments. <sup>b</sup>3 mol % [CuCl(IPr)] used; 61% conversion was observed in the absence of lutidine. <sup>c</sup>Reaction mixture 0.25 M in THF.

diisopropylethylamine (DIPEA), and 2,6-lutidine failed to improve the conversion and similar results were observed in all cases (Table 1, entries 2–4). Interestingly, lutidine actually showed an inhibitory effect when a lower copper loading was used (Table 1, entry 5). On the other hand, 1,10-phenanthroline completely inhibited the cycloaddition reaction (Table 1, entries 6 and 7). It is important to note that phenanthroline has been shown to enhance the reactivity of NHC–copper

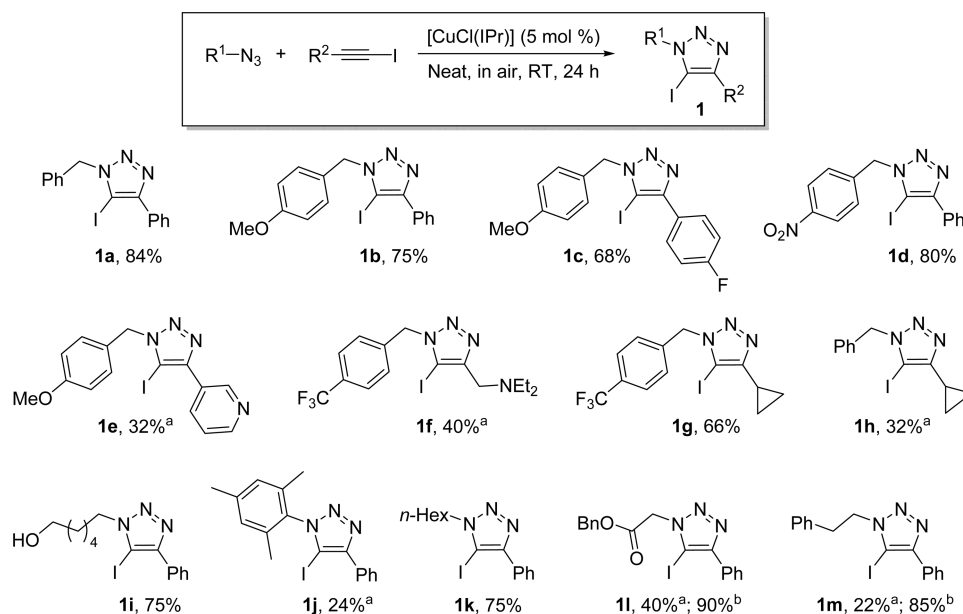
complexes in the cycloaddition reaction of organic azides and terminal alkynes.<sup>23</sup>

In our case, a bright green color was observed when 1,10-phenanthroline was added to the reaction mixture, suggesting oxidation to a copper(II) species, and therefore, to a catalytic dead end. Complexation of the phenanthroline ligand could also be envisaged; however, the reported [CuCl(SIMes)-(phen)] complex is a red compound.<sup>24</sup> No green color was observed when THF was used as solvent, but no triazole product was formed nevertheless.

Next, we attempted to decrease the copper loading, but lower conversions were consistently observed,<sup>25</sup> and a rise in the reaction temperature (from room temperature to 40 °C) led to the decomposition of the starting iodoalkyne. In consequence, 5 mol % [CuCl(IPr)] was used to explore the scope of the reaction (see Scheme 2). Several iodotriazoles could be prepared in good to high yields, including examples bearing electron-rich or electron-poor benzylic chains, alcohol or cyclopropyl groups. On the other hand, bulky substituents and nitrogen-containing functional groups led to low conversions (Scheme 2, compounds **1j**, **1e**, and **1f**). The later observation correlates well with the neutral/negative effect of nitrogen-based additives summarized in Table 1. The use of THF in these sluggish reactions did not improve the reaction conversions. In some cases, however, a very slight increase in copper loading (6 mol %) had a dramatic effect in the reaction conversion (Scheme 2, **1l**, and **1m**). Gratifyingly, in all cases, the prepared triazoles were easily isolated from the reaction mixture after a simple work-up without the need of purification by column chromatography. Furthermore, no formation of dehalogenated triazoles was observed in any of these reactions.

An important advantage of this NHC-based catalytic system is the use of a robust and commercially available copper(I) complex,<sup>26</sup> active under very simple reaction conditions and in the absence of any additive. Moreover, the strength of the copper–NHC bond is of great interest for the study of this

**Scheme 2.** [CuCl(IPr)]-Catalyzed Synthesis of 5-Iodotriazoles (Isolated yields are the average of at least two independent experiments)<sup>a,b</sup>



<sup>a</sup><sup>1</sup>H NMR conversions are the average of at least two independent experiments. <sup>b</sup>Isolated yield with 6 mol % [CuCl(IPr)].

cycloaddition reaction from a mechanistic point of view (see below).

**Copper(I) Complexes Bearing Phosphine Ligands.** Even if other phosphorous ligands have shown to be effective in azide–alkyne cycloaddition reactions,<sup>27</sup> triphenylphosphine has arguably proved to be the most versatile so far.<sup>28</sup> Accordingly, we tested our model reaction with different PPh<sub>3</sub>-containing copper catalysts (see Table 2). Reactions were run neat, since no reaction was observed in either THF, MeCN, toluene, or water.

**Table 2. PPh<sub>3</sub>-Containing Catalysts Screening**

entry	catalyst	conv (%) <sup>a</sup>
1	[CuCl(PPh <sub>3</sub> )]	92 <sup>b</sup>
2	[CuBr(PPh <sub>3</sub> )]	91 <sup>b</sup>
3	[CuCl(PPh <sub>3</sub> ) <sub>3</sub> ]	81
4	[CuBr(PPh <sub>3</sub> ) <sub>3</sub> ]	81
5	[CuI(PPh <sub>3</sub> ) <sub>3</sub> ]	90

<sup>a</sup><sup>1</sup>H NMR conversions are the average of at least two independent experiments. <sup>b</sup>5%–10% of dehalogenated triazole observed by <sup>1</sup>H NMR.

Monophosphine catalysts [CuX(PPh<sub>3</sub>)] led to a good conversion to **1a** (see Table 2, entries 1 and 2); however, <sup>1</sup>H NMR analysis of the reaction mixtures showed a singlet at δ 5.59 ppm, which corresponds to the 5-H-triazole analogue of **1a**.<sup>29</sup> A singlet at δ 3.07 ppm was also observed, indicating that iodoethynylbenzene had been partially dehalogenated to phenylacetylene, which would explain the formation of a 5-H-triazole. Gratifyingly, similar conversions were obtained with the related tris-phosphine complexes (see Table 2, entries 2–4), while no 5-H-triazole was generated even if traces of phenylacetylene were observed in the <sup>1</sup>H NMR spectra of some crude products. Overall, [CuI(PPh<sub>3</sub>)<sub>3</sub>] (see Table 2, entry 5) was selected as the catalyst of choice for efficient and clean reactions.

Next, several nitrogen-containing additives were tested in combination with [CuI(PPh<sub>3</sub>)<sub>3</sub>] (see Table 3). The use of 5 mol % triethylamine or DIPEA had little effect in the reaction conversions (see Table 3, entries 2 and 3). However, 1,10-

**Table 3. Effect of Nitrogen-Containing Additives with [CuI(PPh<sub>3</sub>)<sub>3</sub>]**

entry	additive	conv (%) <sup>a</sup>
1	none	90
2	NEt <sub>3</sub>	84
3	DIPEA	87
4	1,10-phenanthroline	18
5	2,6-lutidine	>95

<sup>a</sup><sup>1</sup>H NMR conversions are the average of at least two independent experiments.

phenanthroline significantly reduced the conversion to iodo-1-phenyl-1H-1,2,3-triazole **1a** (see Table 3, entry 4). This is in agreement with our previous observations with [CuCl(IPr)] as a catalyst (see Table 1); however, in this case, no color change was observed in the reaction mixture.

Pleasantly, the presence of 2,6-lutidine in the reaction mixture resulted in the total conversion of the starting materials into triazoles **1a** (see Table 3, entry 5). The catalyst loading was then optimized using lutidine, but the results obtained in the absence of any additive are also shown for comparative purposes (see Table 4). When the copper loading was

**Table 4. Optimization of [CuI(PPh<sub>3</sub>)<sub>3</sub>] Loading in the Presence of Lutidine**

entry	[Cu] (mol %)	[lutidine] (mol %)	conv (%) <sup>a</sup>
1	5	5	>95 (90)
2	4	5	88 (86)
3	3	5	>95 (84)
4	2	5	>95 (79)
5	1	5	>95 (15)
6	0.5	5	40 (0)
7	0.5	10	8
8	1	50	71
9	1	100	41
10	1	4	>95
11	1	3	69
12	1	1	10

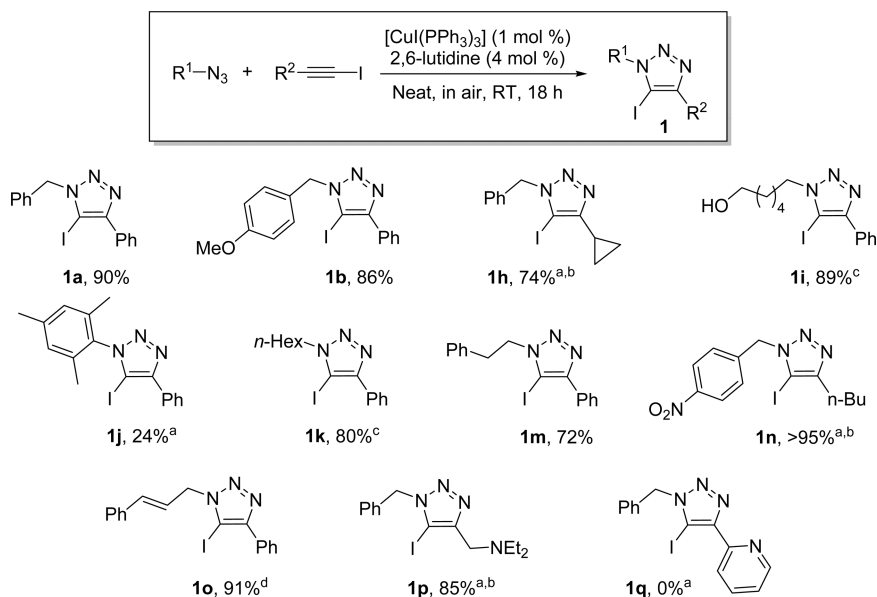
<sup>a</sup><sup>1</sup>H NMR conversions are the average of at least two independent experiments, conversions into brackets were obtained in the absence of 2,6-lutidine.

decreased down to 1 mol %, excellent conversions were still obtained as long as lutidine was present in the reaction mixture. Otherwise, the conversion progressively decreased from 90% to 15% (see Table 4, entries 1–5). Only a moderate conversion into **1a** was obtained with 0.5 mol % [CuI(PPh<sub>3</sub>)<sub>3</sub>] and 5 mol % of lutidine in 24 h, but the reaction still reached completion after 3 days. Increasing the additive loading while keeping the copper one unchanged only led to poorer results (see Table 4, entries 7–9). On the other hand, 4 mol % of 2,6-lutidine could be used without any change in the reaction conversion (see Table 4, entry 10) but a further decrease led to a dramatic reduction in reactivity (see Table 4, entries 11 and 12).

Since only 4 mol % of 2,6-lutidine is required in order to maximize the catalyst efficiency, we hypothesized about the possible formation of a copper–lutidine complex under the reaction conditions. The <sup>1</sup>H and <sup>31</sup>P NMR spectra of a stoichiometric mixture of [CuI(PPh<sub>3</sub>)<sub>3</sub>] and lutidine only showed the signals corresponding to both starting materials and identical results were obtained using [CuI(PPh<sub>3</sub>)] as the copper source instead. Also, no interaction between the additive and either the azide or iodoalkyne was evidenced on NMR. It is important to note that, to the best of our knowledge, despite the numerous CuX–lutidine complexes known, there are no reported examples of these bearing phosphine ligands.<sup>30</sup> Finally, as the formation of dehalogenated phenylacetylene was observed in some reactions (*vide infra*), the intermediacy of



**Scheme 3.**  $[\text{CuI}(\text{PPh}_3)_3]$ -Catalyzed Preparation of 5-Iodotriazoles (Isolated yields are the average of at least two independent experiments)<sup>a,b,c,d</sup>



<sup>a</sup><sup>1</sup>H NMR conversions are the average of at least two independent experiments. <sup>b</sup>Approximately 5% of dehalogenated triazole observed by <sup>1</sup>H NMR. <sup>c</sup>Reaction time = 48 h. <sup>d</sup>Two mol %  $[\text{CuI}(\text{PPh}_3)_3]$ .

an *in situ*-generated *N*-iodolutidinium salt was also investigated. Thus, benzyl azide and phenylacetylene were reacted with one equivalent of *N*-iodolutidinium salt<sup>31</sup> in the presence of 5 mol %  $[\text{CuI}(\text{PPh}_3)_3]$ . However, after 24 h of stirring at room temperature, only traces of iodotriazole **1a** were detected in the reaction mixture. Importantly, no 5-H triazole was produced neither, which indicates that the copper catalyst is not compatible with lutidinium salts under these reaction conditions.

The scope of the optimized catalytic system was finally explored (Scheme 3). In general, similar or better yields were obtained in triazoles **1** when comparing with the  $[\text{CuCl}(\text{IPr})]$ -based catalytic system (see Scheme 2), and, in some cases, the conversions were at least doubled, even if longer reaction times were required (see Scheme 3, **1h** and **1k**). Furthermore, triazoles bearing an alkene or an amine function (see Scheme 3, **1o** and **1p**) could be prepared under these conditions, when only sluggish reactions were obtained with the carbene catalyst. On the other hand, hindered azides and pyridine substituents still led to poor conversions, if any (see Scheme 3, **1j** and **1q**).

The remarkable activity of the phosphine-based complex was sometimes hampered by the formation of small quantities (5%–10%, according to the <sup>1</sup>H NMR spectra) of the corresponding dehalogenated triazoles. When no 5-H-triazole was formed, the expected iodotriazoles **1** were easily isolated after hydrolysis and filtration of the reaction mixture. Overall,  $[\text{CuI}(\text{PPh}_3)_3]$  is an efficient and convenient catalyst for this cycloaddition reaction. Not only does this catalytic system employ, to the best of our knowledge, the lowest copper loading reported for this transformation, but it also relies on an inexpensive and readily prepared catalyst.<sup>32</sup>

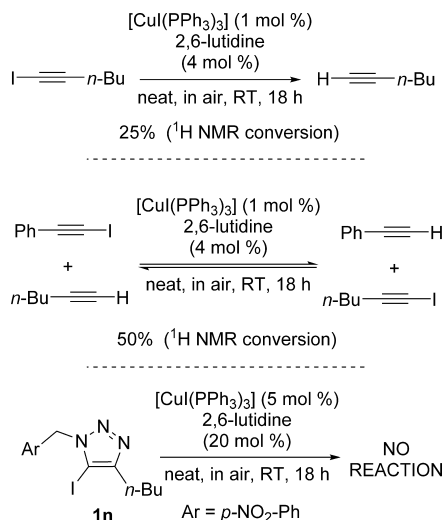
**(B). Mechanistic Studies.** With two optimized catalytic systems based on preformed catalysts in hand, we next carried out combined experimental and computational mechanistic studies on the 1,3-dipolar cycloaddition of azides and iodoalkynes in order to rationalize the observed catalytic effect

and total regioselectivity toward the formation of 5-iodotriazoles.

**Formation of Dehalogenated Triazoles as Byproducts.** The minor formation of 5-H-triazoles in some of our  $[\text{CuI}(\text{PPh}_3)_3]$ -mediated reactions is undesired but not unprecedented. Buckley et al. also observed such byproducts when using a polymeric alkynyl copper(I) catalyst on water under microwave irradiation.<sup>33</sup> In their case, up to 39% of nonhalogenated triazole was obtained. It was then suggested that the 5-H-triazole was generated via the cycloaddition of an *in situ*-generated terminal alkyne upon dehalogenation of the starting iodoalkyne. In order to verify this hypothesis, 1-iodohexyne was subjected to our optimized conditions, and after 18 h of stirring at room temperature (RT), it was found that 25% of the starting alkyne had been transformed to the corresponding terminal alkyne, 1-hexyne (see Scheme 4).<sup>34</sup> Once such dehalogenation starts, it is probable that an equilibrium is then established due to a copper-mediated H/I exchange, as previously reported in the presence of CuI and different amines.<sup>35</sup> To verify this hypothesis, a mixture of the iodoethynylbenzene and 1-hexyne was reacted under identical conditions, and after 18 h of stirring at RT, 50% of 1-hexyne had been converted to 1-iodohexyne. On the other hand, triazole **1n** (see Scheme 3) remained unchanged, even at higher catalyst loadings, indicating the stability of the reaction products (see Scheme 4).

**Computational Procedure.** In this work, the  $\omega$ B97XD density functional theory was used, since it incorporates dispersion interactions to properly model the globular environment, and it has been shown to reproduce reaction barriers effectively.<sup>36</sup> A Def2-SVP basis set was employed, including a pseudopotential for iodine.<sup>37</sup> This results in ~800 basis functions used in the calculation, which is our resource-bound approximate upper limit for a general mechanistic exploration and for calculation of intrinsic reaction coordinates (IRC). All transition states were characterized by normal coordinate analysis, revealing precisely one imaginary mode

## Scheme 4. Control Reactions for the Formation of Dehalogenated Triazoles



corresponding to the intended reaction. In some cases, this was augmented by an IRC calculation, which also established the identity and synchronicity of the reaction. All of the located transition states were found to be stable as a singlet state. Full coordinates for all the stationary points, together with normal-mode animations, are available via Web-Enhanced Tables 1, 2, 3, 4, and 5 (see the individual references for those tables for access), which also include links to full details for each calculation found in a digital repository.<sup>38</sup> Transition states were relocated with inclusion of a self-consistent-reaction-cavity continuum SCRF/CPCM solvation model for dichloromethane, using smoothed reaction cavities for first and second energy derivatives.<sup>39</sup> As the actual reactions were carried out in the absence of solvent, dichloromethane was chosen as a model solvent to approximately model the dielectric of the medium. Unless stated otherwise, all energy values are free energies  $\Delta G_{298}^\ddagger$  (kcal/mol) for a standard state of 1 atm (0.041 M), normalized to a relative free energy of 0 kcal/mol for the isolated reactants. This includes thermal energy correction, including entropy. For a bimolecular reaction, a reduction of  $-2.7$  kcal/mol to the free-energy barrier (not applied in the tables) is required to correct to a standard state of  $\sim 4$  M, the conditions under which the experiments were conducted.<sup>40,41</sup>

In all examined reaction pathways, we used our model reaction of benzyl azide and iodo(ethynylbenzene) and we considered the formation of the corresponding 5-iodo and 4-iodotriazoles **1a** and **2a**, even if the latter was never observed experimentally (Scheme 5). The formation of both regioisomers is strongly exoenergetic, by approximately  $-63$  kcal/mol (see Table 5).

In a first stage,  $\Delta G_{298}^\ddagger$  for the uncatalyzed concerted cycloaddition for both regioisomers were calculated for transition states [3]# and [4]# as 31.4 and 30.2 kcal/mol for the formation of **1a** and **2a**, respectively (34.4 and 31.3 when

Table 5. Free-Energy Profile  $\Delta G_{298}^\ddagger$  of the Uncatalyzed Model Cycloaddition Reaction

compound <sup>a</sup>	$\Delta G_{298}^\ddagger$ (kcal/mol)	digital repository
Az	0.0	10042/to-10287
Alk	0.0	10042/to-10298
[3]#	31.4	10042/to-13966
[4]#	30.2	10042/to-10284
<b>1a</b>	-62.9	10042/24936
<b>2a</b>	-64.6	10042/24933

<sup>a</sup>Species labeled with the suffix “#” correspond to located transition states. See Web-Enhanced Table 1 for an interactive web-enhanced object (WEO) version. Digital repository entries have full details of each calculation, and can be accessed as, e.g., <http://doi.org/10042/24933>.

the solvation model is applied; see Table 5 and Web-Enhanced Table 1). Since experimentally no reaction was observed at room temperature in the absence of a copper catalyst, pathways with transition states that have  $\Delta G_{298}^\ddagger$  values higher than  $\sim 30$  kcal/mol were not pursued any further.

**Active Copper Species in the Cycloaddition of Azides and Iodoalkynes.** The use of ligands is crucial in the cycloaddition of azides and iodoalkynes. Examples have been reported where the catalytically active species were generated *in situ* upon reaction of the chosen copper source and ligand precursors,<sup>7,11</sup> or alternatively, from a well-defined complex.<sup>8</sup> Whereas the *in situ* strategy avoids the need to preisolate any metallic species, the use of preformed catalysts generally avoids the need for excess of ligands and/or reagents for achieving optimal catalytic performance and allows for a better control of the nature of the species present in the reaction media.<sup>42</sup> In most cases, however, the complex used is a precatalyst, rather than the actual active species. Hence, we tried to determine the most likely active species generated from either  $[\text{CuCl}(\text{IPr})]$  or  $[\text{Cu}(\text{PPh}_3)_3]$ .

In the case of  $[\text{CuCl}(\text{IPr})]$ , the strength of the metal–NHC bond<sup>43</sup> and the mild reaction conditions used were expected to ensure the structural integrity of the catalyst. This was confirmed by the  $^1\text{H}$  NMR analysis of the crude reaction mixtures. Accordingly, we used  $[\text{CuCl}(\text{IPr})]$  in our theoretical calculations.

For the phosphine-based reactions, it is important to note that the exact nature of  $\text{CuX}/\text{phosphine}$  systems in solution is very difficult to predict, since not only ligand decoordination, but also the formation of polynuclear species through halogen bonding must be taken into account.<sup>44</sup> Also, it is not possible to extrapolate the literature results to our system since the cycloaddition reactions were performed under neat conditions, which will affect the nature of the formed species from the starting catalytic system. On the other hand, since we could not experimentally clarify the role of lutidine in the  $[\text{Cu}(\text{PPh}_3)_3]$ -mediated cycloaddition reactions and the catalytic reactions proceeded as well in the absence of this additive, lutidine was not included in the following experiments or in the computational studies. This also allows comparison of the computational results obtained for the  $\text{PPh}_3$  and  $\text{IPr}$  systems, since lutidine did not improve the performance of the latter (see Table 1).

We first ran a series of experiments with different amounts of  $\text{CuI}$  and free triphenylphosphine. As expected, no reaction occurred in the absence of any ligand (see Table 6, entry 1),<sup>45</sup> whereas, among all the *in situ*-generated systems, the best conversion was obtained when 10 mol %  $\text{PPh}_3$  (1:2 copper/

## Scheme 5. Model Reaction for Computational Studies

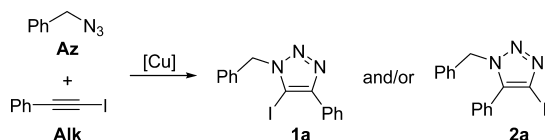


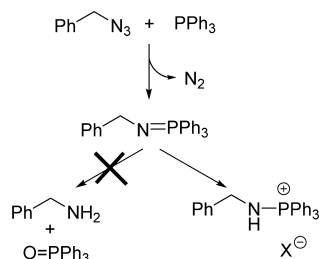
**Table 6.** *In Situ*-Generated PPh<sub>3</sub>-Containing Catalysts

$\text{Ph}-\text{N}_3 + \text{Ph}-\text{C}\equiv\text{I} \xrightarrow[\text{Neat, in air, RT, 24 h}]{\text{CuI (5 mol \%), PPh}_3 \text{ (X mol \%)}} \text{Ph}-\text{N}=\text{N}-\text{C}(\text{Ph})=\text{C}(\text{Ph})-\text{I}$		
entry	PPh <sub>3</sub> (mol %)	conv (%) <sup>a</sup>
1	0	0
2	5	41
3	10	81
4	15	70
5	20	<5
6 <sup>b</sup>	0	90
7 <sup>b</sup>	5	85

<sup>a</sup><sup>1</sup>H NMR conversions are the average of at least two independent experiments. <sup>b</sup>[CuI(PPh<sub>3</sub>)<sub>3</sub>] (5 mol %) used instead of CuI.

ligand ratio) was used (see Table 6, entry 3). Higher phosphine loadings had a deleterious effect on the reaction, which might also be due to inefficient mixing under neat conditions (Table 6, entries 4 and 5). Overall, the preformed complex [CuI(PPh<sub>3</sub>)<sub>3</sub>] remained the best performing catalyst in the series (Table 6, entry 6).

Furthermore, the presence of significant amounts of free phosphine in the reactions is expected to lead to the formation of the corresponding iminophosphorane issue of the Staudinger reduction of benzyl azide.<sup>46</sup> Because of the presence of moisture in the reaction mixture, this phosphorane should be hydrolyzed to benzylamine and triphenylphosphine oxide (see Scheme 6). However, when the model reaction was run in the

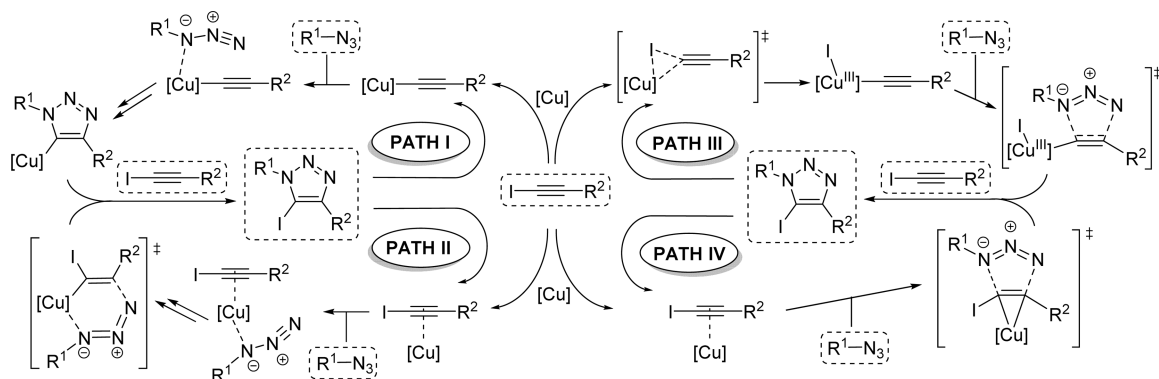
**Scheme 6.** Undesired Reactivity Observed with Free PPh<sub>3</sub>

presence of 5 mol % of CuI and 15 mol % of PPh<sub>3</sub> (see Table 6, entry 4), the appearance of a new multiplet at 4.29 ppm was observed, but no traces of benzylamine were detected on the

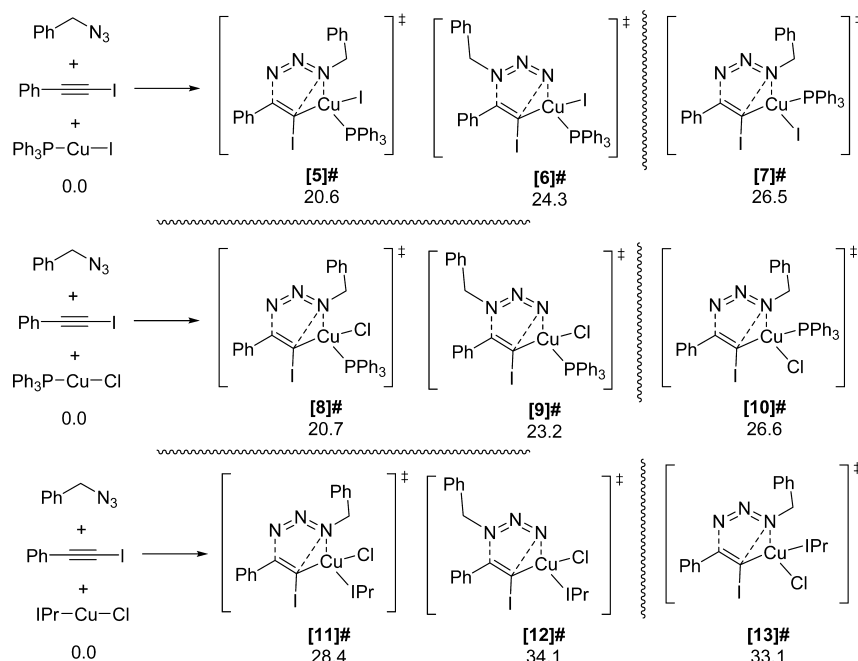
<sup>1</sup>H NMR. Moreover, the <sup>31</sup>P NMR spectrum only showed two sharp signals at 29.9 and 39.2 ppm, respectively (ratio = 3:2).<sup>47</sup> The first one corresponds to triphenylphosphine oxide, and the second one, which is too far downfield for an iminophosphorane, was attributed to a phosphonium salt, based on similar/identical chemical shifts of benzylaminophosphonium salts reported in the literature (Scheme 6).<sup>48</sup> In our case, the most likely counterion for such a salt is iodide resulting from the partial dehalogenation of the starting iodoalkyne, as traces of phenylacetylene were also observed in the crude reaction products. This undesired reaction appeared to be particularly active when using monophosphine complexes as catalysts (see Table 2).

When the model reaction was carried out with 5 mol % of [CuI(PPh<sub>3</sub>)<sub>3</sub>], the <sup>31</sup>P NMR spectrum of the reaction mixture did not present the signals corresponding to the starting catalyst, its monophosphine analogue, or PPh<sub>3</sub>. Instead, the spectrum showed that triphenylphosphine oxide was the major phosphorus-containing compound, as well as the formation of two unknown minor products at 9.6 and 6.6 ppm.<sup>45</sup> These results seem to suggest that [CuI(PPh<sub>3</sub>)<sub>3</sub>] is not the actual catalyst in the cycloaddition reaction but also, that all PPh<sub>3</sub> molecules play an important role in the catalytic cycle, maybe stabilizing more-reactive species. This would avoid their decomposition and a consequent loss of activity, since they are not available for reacting with benzyl azide. Taking into account these observations, [CuI(PPh<sub>3</sub>)] was chosen as the catalyst in our computational studies. For comparative purposes, some of the calculations were also carried out with [CuCl(PPh<sub>3</sub>)]. Not only was this catalyst shown to be active in the preliminary screening (see Table 2), it also represents a useful link to assess the effect of changing either a L or a X ligand from [CuI(PPh<sub>3</sub>)] to [CuCl(IPr)].

**Plausible Catalytic Cycles.** Two reaction pathways have been previously proposed for the cycloaddition reaction of azides and iodoalkynes, both heavily based on previous evidence for the cycloaddition of azides and terminal alkynes (see Scheme 7).<sup>4,16,49</sup> Path I would initiate with the formation of a  $\sigma$ -acetylide species. This is a well-established intermediate in the cycloaddition of azides and terminal alkynes, and therefore from here, the reaction would undergo the broadly accepted sequence with monosubstituted alkynes. The eventual reaction of a triazolide intermediate with the starting iodoalkyne would generate the expected product and close the catalytic cycle.<sup>50</sup> In Path II, the starting iodoalkyne would

**Scheme 7.** Overview of Mechanistic Pathways for the Cycloaddition Reaction<sup>a</sup>

<sup>a</sup>[Cu] denotes a ligated copper(I) center, unless indicated otherwise.

Scheme 8. Located  $\text{Cu}^{\text{III}}$  Transition States<sup>a</sup>

<sup>a</sup>Values shown are for  $\Delta G_{298}$  and are given in units of kcal/mol.

be  $\pi$ -coordinated by the copper catalyst before interacting with the azide,<sup>51</sup> which would lead to the formation of a vinylidene 6-membered cyclic species that would produce the expected triazoles upon reaction with a molecule of iodoalkyne (see Scheme 7). A very significant difference between both proposals is that, in Path II, the C–I bond is not severed during the catalytic cycle. Triazolides are known to be extremely sensitive to the presence of proton sources<sup>52</sup> and, therefore, unsuitable intermediates in this reaction. A 5-H-triazole should indeed be the only reaction product under technical conditions, should the reaction proceed via a triazolide intermediate.<sup>53</sup>

In addition to Path II, we have also investigated two other alternatives: Paths III and IV (Scheme 7). Path III would involve the oxidative addition of the iodoalkyne onto the copper catalyst, followed by the cycloaddition step and a reductive elimination. Path IV is based on the direct activation of the iodoalkyne via  $\pi$ -coordination to the copper center.

**Path II ( $\text{Cu}^{\text{III}}$  Metallacycles).** Using our level the theory and  $[\text{CuI}(\text{PPh}_3)]$  as the catalyst, we were able to locate not only [5]#, leading to formation of the observed 5-iodotriazole, but also the regioisomeric [6]# (see Scheme 8, Table 7 and Web-Enhanced Table 2). Transition state [5]# is 4 kcal/mol lower in  $\Delta G_{298}^\ddagger$  than [6]# (20.6 and 24.3 kcal/mol, respectively, for gas phases). This difference in energy can account for the complete regioselectivity observed experimentally, even if it is much smaller than that previously found in calculations with terminal alkynes (i.e., 13 kcal/mol in favor for the formation of 5-H-triazoles).<sup>54</sup> The relative configuration of the copper center was found to be very important as a transition state [7]# leading to the formation of **1a** but presenting both halogen atoms on the same side of the transition state, was significantly higher in energy, even higher than regioisomeric [6]#. The transition states leading to the formation of **1a** located with  $[\text{CuCl}(\text{PPh}_3)]$  as the catalyst, [8]#–[10]#, displayed a free energy very similar to that corresponding to [5]#–[7]# (see Scheme

**Table 7. Free-Energy Profile  $\Delta G_{298}^\ddagger$  for the Formation of Iodotriazoles via a  $\text{Cu}^{\text{III}}$  Metallacycle<sup>a</sup>**

compound <sup>b</sup>	$\Delta G$ (kcal/mol)	digital repository
$[\text{CuI}(\text{PPh}_3)]$	0.0	10042/24798
$[\text{CuCl}(\text{PPh}_3)]$	0.0	10042/25072
$[\text{CuCl}(\text{IPr})]$	0.0	10042/24997
[5]#	20.6	10042/25071
[6]#	24.3	10042/24601
[7]#	26.5	10042/24668
[8]#	20.7	10042/24488
[9]#	23.2	10042/29498
[10]#	26.6	10042/29027
[11]#	28.4	10042/24666
[12]#	34.1	10042/24831
[13]#	33.1	10042/24843

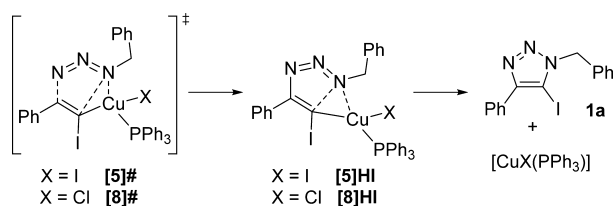
<sup>a</sup>See Web-Enhanced Table 2 for an interactive WEO version. <sup>b</sup>Species labeled with the suffix “#” correspond to located transition states.

8, Table 7, and Web-Enhanced Table 2). These results correlate well with the experimental catalyst screening (see Table 2), where a change of the halogen on the copper catalyst led only to slightly different performances.

Similar calculations with  $[\text{CuCl}(\text{IPr})]$  as catalyst revealed that the barrier in this case slightly higher ([11]#, 28.4 kcal/mol), but this transition state is considerably stabilized when compared to [13]# as well as compared to its regioisomer leading to the formation of a 4-I-triazole **2a** ([12]#, 34.1 kcal/mol) (see Scheme 8 and Table 7).

Intrinsic reaction coordinate (IRC) computations were run from geometries [5]# and [8]# to further validate this mechanistic pathway. These showed two interesting features (see Scheme 9, Web-Enhanced Table 2, and Figure 2). First, no  $\pi$ -coordination of the alkyne is involved prior the formation of [5]# or [8]#, as had been previously proposed,<sup>7</sup> and the copper catalyst interacts with benzyl azide instead.



**Scheme 9. Intrinsic Reaction Coordinate (IRC) Path from Transition State to Products**


Both before and after the transition states, features appeared in the gradient norm characteristic of a so-called hidden intermediate in the reaction (Figure 2b, red arrows). A hidden intermediate (it could also be called a frustrated intermediate) is not expected to have a lifetime longer than a molecular vibration, but it could potentially be converted to a real intermediate if the reaction conditions or the substitution pattern are changed.<sup>55</sup> In our case, at IRC = 2.5, the hidden intermediates [5]HI and [8]HI (where the suffix “HI” denotes hidden intermediate) can be found for the formation of the second C–N bond (I–C···N–Bn), which is concomitant with the reductive elimination of the copper to form the triazole product. Hence, both the cycloaddition and the elimination are part of the same concerted process, albeit occurring asynchronously. Furthermore, a second hidden intermediate emerged before [5]#, corresponding to an agostic interaction between the copper center and the alkyne C–I bond.

**Path III (Oxidative Addition of the Iodoalkyne).** The oxidative addition of haloalkynes onto copper(I) centers has already been evoked for transformations such as the Cadiot–Chodkiewicz coupling of 1-haloalkynes with terminal alkynes,<sup>56,57</sup> but not for this type of cycloaddition reaction. We explored this possibility but we were unable to locate any transition state leading to the observed **1a**.

On the other hand, the energy of the found transition states [14]# and [15]# for the formation of 4-iodotriazole **2a** was greater in magnitude than the uncatalyzed thermal process by ~45 kcal/mol (see Scheme 10 and Web-Enhanced Table 2). In consequence, this sequence was not studied any further.

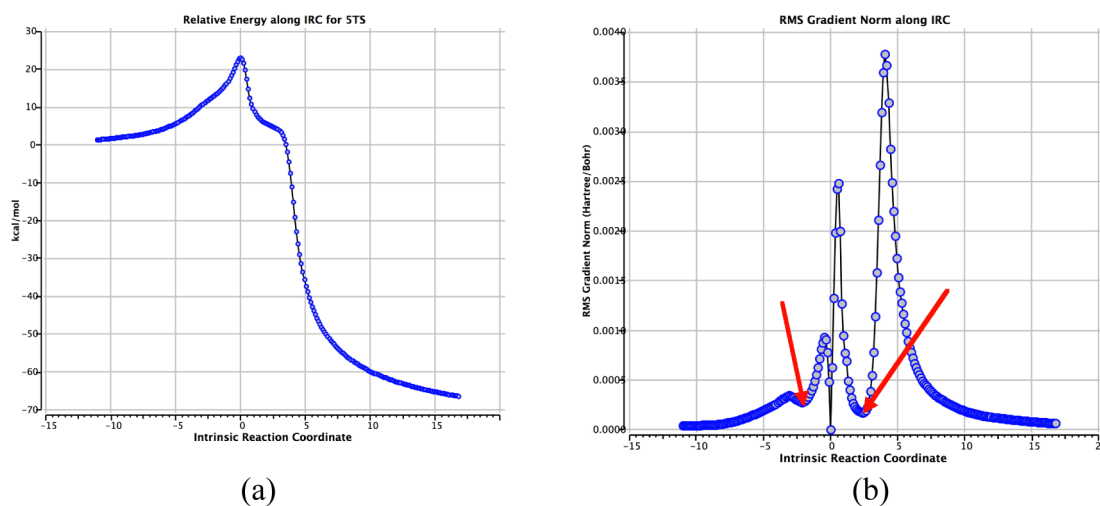
**Path IV (Direct Activation via  $\pi$ -Coordination of the Iodoalkyne).** Copper(I) alkyne  $\pi$ -complexes have long been considered essential intermediates in the cycloaddition of azides and alkynes (either terminal or halogenated).<sup>47</sup> However, the cycloaddition of terminal alkynes via  $\pi$ -coordination of the alkyne without its deprotonation has been found to be higher in energy than the uncatalyzed reaction.<sup>47</sup> We decided to assess this type of mechanism with iodoalkynes, since both cycloaddition reactions show significant differences (see Schemes 11 and 12, Table 8, and Web-Enhanced Table 3).

From the phosphine catalyst and the model iodoalkyne, two regioisomeric  $\pi$ -complexes **16** and **17** can be formed. Both compounds have similar free energies (−2.1 and 0.1 kcal/mol, respectively); their formation is exothermic ( $\Delta H \approx 15$  kcal/mol), but this is negated by a loss of entropy. The reaction of **16** with benzyl azide led to transition state [18]#, which is a precursor of a 5-iodotriazole **1a** and is only 19.6 kcal/mol above the starting materials, with regard to free energy. Moreover, its regioisomer [19]# is 5 kcal/mol higher in energy and a transition state [20]# leading to **1a**, but issue of the reaction of  $\pi$ -complex **17** displayed an equally high energy (see Scheme 11).

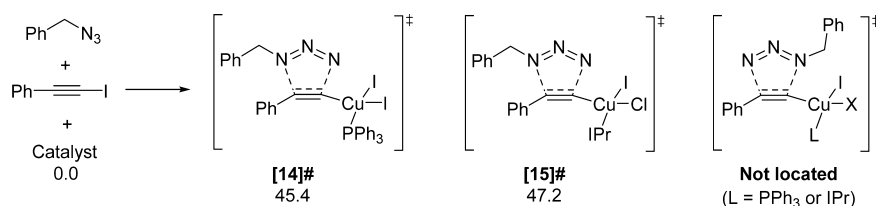
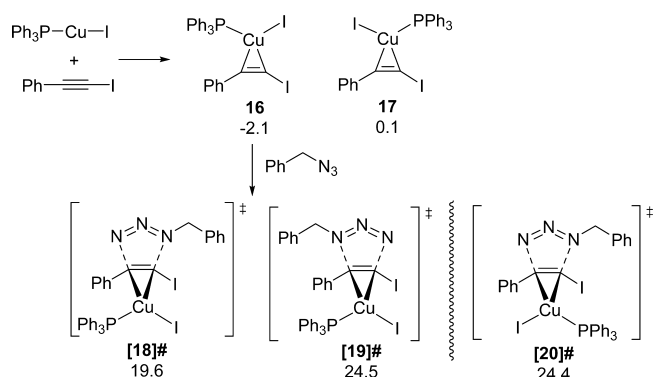
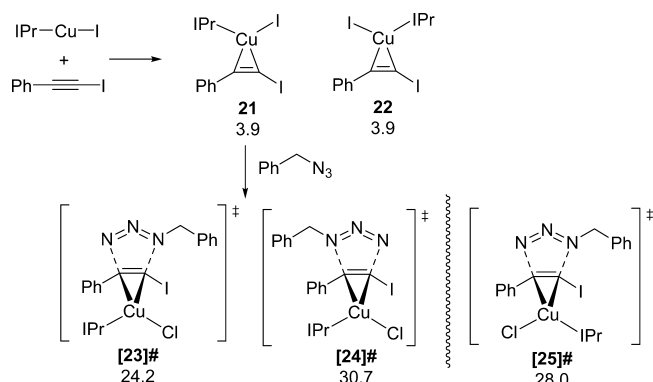
Very similar results were obtained with [CuCl(IPr)] as the catalyst, and even if [23]# has a higher energy of 24.2 kcal/mol, this remains the lowest transition state located with the NHC system. Although this value of energy seems slightly high for reactions operating at RT, it should be taken into account that the −2.7 kcal/mol correction for a standard state of ~4 M (the actual reaction conditions) is not applied in any of the tables (*vide supra*).

Furthermore, the NHC-based system is particularly complex, from a conformational point of view. Thus, calculations using a model catalyst led to a transition state at 22.5 kcal/mol, with respect to the starting materials while showing the same trend in the relative energy values between transition states [26]#, [27]#, and [28]#, when compared to the analogous compounds [23]#, [24]#, and [25]#, respectively (see Scheme 13, Table 9).

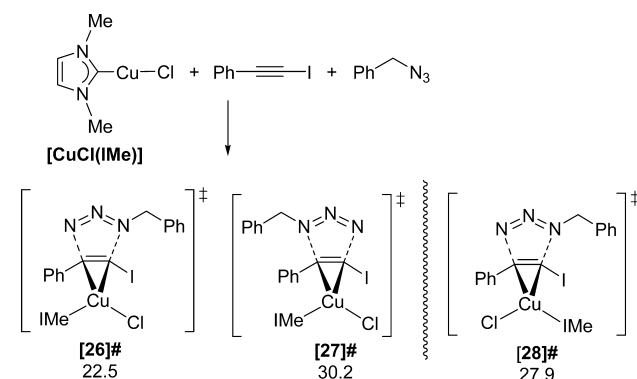
IRC computations run from geometry [18]# further validated this mechanistic pathway via a  $\pi$ -activation of the iodoalkyne. Also, a hint of the occurrence of a hidden



**Figure 2.** Calculated intrinsic reaction coordinate for [5]#, showing (a) the relative energy and (b) the computed gradient norm. For the latter, red arrows indicate the occurrence of hidden reaction intermediates. The same features are also visible in the IRC computed with a continuum solvent field.

Scheme 10. Calculated Energy Barriers for the Cycloaddition Reaction after Oxidative Addition<sup>a</sup><sup>a</sup>Values shown are for  $\Delta G_{298}$  and are given in units of kcal/mol.Scheme 11. Direct  $\pi$ -Activation with [CuI(PPh<sub>3</sub>)]<sup>a</sup><sup>a</sup>Values shown are for  $\Delta G_{298}$  and are given in units of kcal/mol.Scheme 12. Direct  $\pi$ -Activation with [CuCl(IPr)]<sup>a</sup><sup>a</sup>Values shown are for  $\Delta G_{298}$  and are given in units of kcal/mol.Table 8. Free-Energy Profile  $\Delta G_{298}^\ddagger$  for the Formation of Iodotriazoles via Direct  $\pi$ -Activation<sup>a</sup>

compound <sup>b</sup>	$\Delta G$ (kcal/mol)	digital repository
16	-2.1	10042/25672
17	0.1	10042/24673
[18]#	19.6	10042/24844
[19]#	24.5	10042/24838
[20]#	24.4	10042/24834
21	3.9	10042/24925
22	3.9	10042/24923
[23]#	24.2	10042/25040
[24]#	30.7	10042/24914
[25]#	28.0	10042/24934

<sup>a</sup>See Web-Enhanced Table 3 for an interactive WEO version. <sup>b</sup>Species labeled with the suffix “#” correspond to located transition states.Scheme 13. Direct  $\pi$ -Activation with Model [CuCl(IME)]<sup>a</sup><sup>a</sup>Values shown are for  $\Delta G_{298}$  and are given in units of kcal/mol.Table 9. Free-Energy Profile  $\Delta G_{298}^\ddagger$  for the Formation of Iodotriazoles with Model Systems<sup>a</sup>

compound <sup>b</sup>	$\Delta G$ (kcal/mol)	digital repository
[CuCl(IME)]	0.0	10042/27425
[26]#	22.5	10.6084/m9.figshare.936558
[27]#	30.2	10.6084/m9.figshare.928087
[28]#	27.9	10042/27461
[29]#	27.0	10042/24926
[30]#	30.1	10042/24665
MeN <sub>3</sub>	0.0	10.6084/m9.figshare.1022870
MeCCI	0.0	10.6084/m9.figshare.1022871
[CuI(PMe <sub>3</sub> )]	0.0	10042/29032
[31]#	21.9	10042/29366
[32]#	24.7	10042/29239

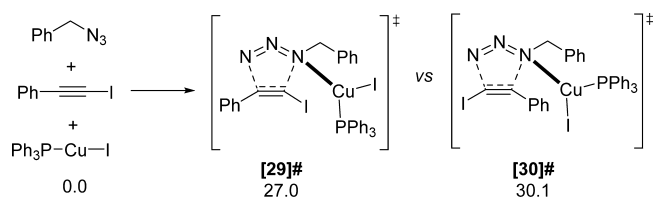
<sup>a</sup>See Web-Enhanced Table 4 for an interactive WEO version. <sup>b</sup>Species labeled with the suffix “#” correspond to located transition states.

intermediate could be found. This corresponds to the formation of a copper(I)  $\pi$ -complex with the final triazole product.<sup>47</sup>

For completeness, the coordination of benzyl azide to the copper center prior to any interaction with the alkyne was also investigated. From the phosphine-containing catalyst, two regioisomeric transition states [29]# and [30]# could be located (see Scheme 14 and Table 9). The free-energy barriers are 27 and 30 kcal/mol, respectively, in favor of [29]#, leading to the 5-iodotriazole that is obtained experimentally. However, the computed energy values are significantly higher than those reported for Paths II and IV (20.6 and 19.6 kcal/mol, respectively).

An IRC computation was run from geometry [29]# to validate this mechanistic pathway. It is important to note that no intermediates are involved in this path, and also that no interaction of the alkyne with the copper catalyst occurred once

### Scheme 14. Calculated Energy Barriers for the Cycloaddition Reaction via Azide Activation<sup>a</sup>

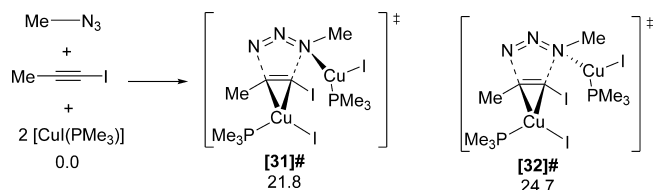


<sup>a</sup>Values shown are for  $\Delta G_{298}$  and are given in units of kcal/mol. See Web-Enhanced Table 4 for an interactive WEO version.

the N atom of the azide bearing the benzyl group coordinates with the metal (see Web-Enhanced Table 4).

Nevertheless, the interaction of the catalyst with the organic azide led to a decrease of  $\sim 3$  kcal/mol in the free energy of activation, when compared to the metal-free thermal reaction (see Table 5). We then extended the model to a study of binuclear paths, since these are well-established for the cycloaddition of azides and terminal alkynes.<sup>58</sup> These calculations, carried out on a model system, led to the location of transition states [31]# and [32]# in which two different copper centers activate each cycloaddition partner (see Scheme 15, Table 9, and Web-Enhanced Table 4). A Cu–Cu

### Scheme 15. Calculated Energy Barriers for a Binuclear Path<sup>a</sup>



<sup>a</sup>Values shown are for  $\Delta G_{298}$  and are given in units of kcal/mol. See Web-Enhanced Table 4 for an interactive WEO version.

interaction seems important for the viability of these bimetallic species, as [31]# displayed a Cu–Cu separation of 2.69 Å, with this value being shorter than the sum of the van der Waals radii (2.80 Å). In contrast, [32]#, where no such interaction is present because the Cu atoms are on opposite sides of the reactants, is higher in energy.

When compared to our previous results, [31]# and [32]# are actually higher in free energy than the preceding mononuclear transition state (21.8 and 24.7 kcal/mol, compared to 20.6 kcal/mol for [5]#; see Scheme 11). A more complete exploration of multinuclear coordination is deferred to a future report on this mechanism; clearly further studies are required to determine the order of the reaction in [Cu] under the given conditions.

**Visualization of the Origins of Transition-State Stability.** A valuable adjunct to the computed relative (free) energies of isomeric transition states is some method of probing their origins. In general terms, these differences arise from a combination of bond-centered covalent terms and the so-called noncovalent interactions (NCIs).<sup>59</sup> Any such analysis is almost invariably complex, since it often arises from the addition of a large number of small terms rather than from one single effect. We have recently explored the application of a convenient visual presentation of just the noncovalent (or NCI) regions, those arising from weak interactions such as hydrogen bonds, electrostatic effects and dispersion forces. The importance of

obtaining models in which dispersion terms are included in the Hamiltonian has previously been noted,<sup>60</sup> which, in our study, are conveniently built into the  $\omega$ B97XD DFT. It has been recently shown<sup>59</sup> that a computed quantity known as the reduced density gradient (RDG) can be used to reveal noncovalent interactions present in the system, allowing rapid visual identification and characterization of weak interactions of various strengths as chemically intuitive RDG isosurfaces. These are color-coded to reveal stabilizing hydrogen bonds in blue, weaker van der Waals attractions in green, and destabilizing interactions (such as steric clashes) in red, with weaker ones in yellow. Such a color-coded RDG isosurface for [18]# (the lowest energy transition state of several isomeric possibilities, see Scheme 11) is shown in Figure 3 (the

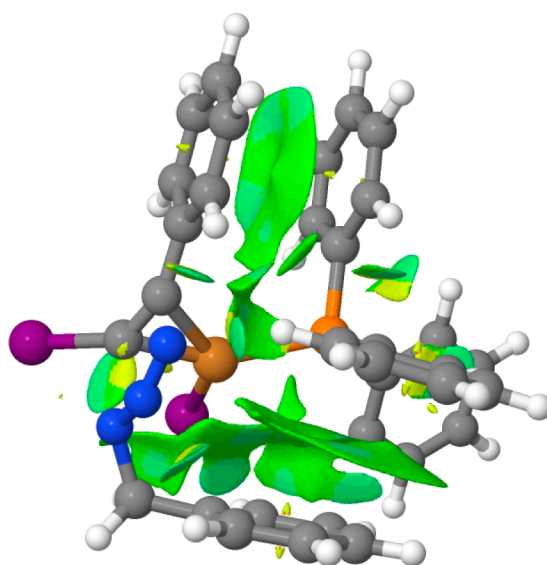


**Figure 3.** NCI (noncovalent interaction) surface for [18]#. The green regions reveal the zones of attractive dispersion forces corresponding to  $\pi$ -stacking, and the pale blue ones show other stabilizing regions.

interactive version of this also includes such an analysis for the isomeric transition states [19]# and [20]# in Web-Enhanced Table 5). This clearly shows the strong effect of  $\pi$ -stacking dispersion stabilizations in a system rich in phenyl groups. While any individual stacking interaction may only contribute  $\sim 1$ – $2$  kcal/mol to the overall stability, the effect rapidly accumulates for the system as a whole. The overall stability of any given isomeric transition state is clearly a combination of such interactions and the stronger covalent interactions. A more-detailed analysis in which a spline of the RDG values can be integrated<sup>60</sup> to enable a comparison of the noncovalent interactions in stereoisomeric systems (for which the covalent contributions might be expected to largely cancel) will be reported elsewhere.

## CONCLUSION

We have developed two competent catalytic systems for the 1,3-dipolar cycloaddition of organic azides and iodoalkynes. These rely on economical and easily accessible copper complexes, which is expected to assist their widespread application. Mechanistic studies, and in particular DFT calculations indicate that two different mechanisms are possible for this reaction and they might be competitive: either formation of a copper(III) metallacycle or the direct activation

of the iodoalkyne via  $\pi$ -coordination of the copper catalyst. Importantly, these mechanisms accounts both for the catalyst-acceleration effect in this cycloaddition reaction and the exclusive regioselectivity of the copper-catalyzed version toward the formation of 5-iodotriazoles.

Our results are evidence of key differences between the reactions of terminal and halogenated alkynes under copper catalysis conditions. Hence, neither of the proposed mechanistic options involves the intermediacy of copper-acetalide species, which are well-accepted intermediates in the cycloadditions of terminal alkynes. This is well-aligned with the work of Fokin and co-workers, which suggests that cleavage of the C–I bond is not required for the cycloaddition to take place, and, as a consequence, the copper catalyst would interact with the substrates through  $\pi$ -interactions.<sup>58</sup> At this stage, mononuclear mechanisms remain a viable route, although alternative binuclear or trinuclear mechanisms cannot be excluded.

To the best of our knowledge, this is the first computational study reported for this particular cycloaddition reaction. We consider that better mechanistic understanding of this reaction is essential for it to have the same impact as the cycloaddition of terminal alkynes and azides (often referred to as the cream of the crop in Click chemistry). In particular, the possibility of undergoing a cycloaddition via a direct  $\pi$ -activation of the alkynes opens up the prospect of reacting iodoalkynes with a variety of dipoles other than azides. This, together with further mechanistic investigations, is currently underway and will be reported in due course.

## EXPERIMENTAL SECTION

**CAUTION:** Although we did not experience any problems, the cycloaddition of azides and iodoalkynes is highly exothermic and, as a consequence, adequate cooling should always be available when performing the reaction in the absence of solvent.

**(A). [3 + 2] Cycloaddition of Azides and Iodoalkynes with [CuCl(IPr)].** In a vial fitted with a screw cap, [CuCl(IPr)] (12 mg, 5 mol %), azide (0.5 mmol), and iodoalkyne (0.5 mmol) were loaded. The reaction was allowed to proceed at room temperature for 24 h. Then, saturated aq. ammonium chloride solution (10 mL) was added and the resulting mixture was stirred vigorously for 3 h. The resulting precipitate was filtered and washed with water and pentane. In all examples, the crude products were estimated to be >95% pure by <sup>1</sup>H NMR. Reported yields are isolated yields and are the average of at least two independent experiments.

**(B). [3 + 2] Cycloaddition of Azides and Iodoalkynes with [CuI(PPh<sub>3</sub>)<sub>3</sub>].** In a vial fitted with a screw cap, [CuI(PPh<sub>3</sub>)<sub>3</sub>] (5 mg, 1 mol %), 2,6-lutidine (3  $\mu$ L, 4 mol %) azide (0.5 mmol) and iodoalkyne (0.5 mmol) were loaded. The reaction was allowed to proceed at room temperature for 18 h. Then, saturated aqueous ammonium chloride solution (10 mL) was added and the resulting mixture was stirred vigorously for 3 h. The resulting precipitate was filtered and washed with water and pentane. In all examples, the crude products were estimated to be >95% pure by <sup>1</sup>H NMR. Reported yields are isolated yields and are the average of at least two independent experiments.

## ASSOCIATED CONTENT

### Supporting Information

Experimental procedures and characterization data. This material is available free of charge via the Internet at <http://pubs.acs.org>. The Web-Enhanced Tables embedded in the HTML version of this article can also be accessed through the following DOI links. **Web-Enhanced Table 1:** Free energy profile of the uncatalyzed model  $\pi$ 2s +  $\pi$ 4s cycloaddition reaction (<http://dx.doi.org/10.6084/m9.figshare.865637>).

**Web-Enhanced Table 2:** Free-energy profile of the formation of iodotriazoles via a copper(III) metallacycle pathway (Paths II and III) (<http://dx.doi.org/10.6084/m9.figshare.865638>).

**Web-Enhanced Table 3:** Free-energy profile for the formation of iodotriazoles via a Cu-catalyzed cycloaddition pathway (Path IV) (<http://dx.doi.org/10.6084/m9.figshare.865639>); **Web-Enhanced Table 4:** Free-energy profile for the formation of triazoles with model systems (<http://dx.doi.org/10.6084/m9.figshare.1029169>).

**Web-Enhanced Table 5:** Noncovalent-interaction (NCI) surfaces for selected transition states (<http://dx.doi.org/10.6084/m9.figshare.1030188>).

## AUTHOR INFORMATION

### Corresponding Author

\*Tel.: (+44) 207579 49699. E-mail: [s.diez-gonzalez@imperial.ac.uk](mailto:s.diez-gonzalez@imperial.ac.uk).

### Notes

The authors declare no competing financial interest.

## ACKNOWLEDGMENTS

We gratefully acknowledge Imperial College London and EPSRC for financial support.

## ABBREVIATIONS

IPr = *N,N'*-bis(2,6-diisopropylphenyl)imidazol-2-ylidene; SIPr = *N,N'*-bis(2,6-diisopropylphenyl)imidazolin-2-ylidene; IMes = *N,N'*-bis(2,4,6-trimethylphenyl)imidazol-2-ylidene; SIMes = *N,N'*-bis(2,4,6-trimethylphenyl)imidazolin-2-ylidene; IAd = *N,N'*-diadamantylimidazol-2-ylidene

## REFERENCES

- (1) Huisgen, R. *Pure Appl. Chem.* **1989**, 61, 613–628.
- (2) (a) Tornøe, C. W.; Christensen, C.; Meldal, M. *J. Org. Chem.* **2002**, 67, 3057–3064. (b) Rostovtsev, V. V.; Green, L. G.; Fokin, V. V.; Sharpless, K. B. *Angew. Chem., Int. Ed.* **2002**, 41, 2596–2599.
- (3) (a) Special issue on Click chemistry, *Chem. Soc. Rev.* **2010**, 39, 1221–1408. (b) For a comprehensive review, see: Meldal, M.; Tornøe, C. W. *Chem. Rev.* **2008**, 108, 2952–3015. (c) *Click Chemistry for Biotechnology and Materials Science*; Lahann, J., Ed.; Wiley: Chichester, U.K., 2009.
- (4) (a) Berg, R.; Straub, B. F. *Beilstein J. Org. Chem.* **2013**, 9, 2715–2750. (b) Bock, V. D.; Hiemstra, H.; van Maarseveen, J. H. *Eur. J. Org. Chem.* **2006**, 51–68.
- (5) (a) Díez-González, S.; Correa, A.; Cavallo, L.; Nolan, S. P. *Chem.–Eur. J.* **2006**, 12, 7558–7564. (b) Candelon, N.; Lastécouères, D.; Diallo, A. K.; Aranzaes, J. R.; Astruc, D.; Vincent, J. M. *Chem. Commun.* **2008**, 741–743.
- (6) Kuijpers, B. H. M.; Dijkmans, G. C. T.; Groothuys, S.; Quaedflieg, P. J. L. M.; Blaauw, R. H.; van Delft, F. L.; Rutjes, F. P. J. T. *Synlett* **2005**, 3059–3062.
- (7) Hein, J. E.; Tripp, J. C.; Krasnova, L. B.; Sharpless, K. B.; Fokin, V. V. *Angew. Chem., Int. Ed.* **2009**, 48, 8018–8021. For one earlier copper-free (and non regioselective) example using ionic liquids as reaction medium. See: Zhong, P.; Guo, S.-R. *Chin. J. Chem.* **2004**, 22, 1183–1186.
- (8) (a) García-Álvarez, J.; Díez, J.; Gimeno, J. *Green Chem.* **2010**, 12, 2127–2130. (b) García-Álvarez, J.; Díez, J.; Gimeno, J.; Suárez, F. J.; Vincent, C. *Eur. J. Inorg. Chem.* **2012**, 5854–5863.
- (9) Buckley, B. R.; Dann, S. E.; Heaney, H. *Chem.–Eur. J.* **2010**, 16, 6278–6284.
- (10) For a recent report on the iridium-mediated synthesis of 4-bromotriazoles, see: Rasolofonjatovo, E.; Theeramunkong, S.; Bouriaud, A.; Kolodych, S.; Chaumontet, M.; Taran, F. *Org. Lett.* **2013**, 15, 4698–4701.



- (11) For reactions carried out with a copper tubing/TTTA combination, see: Bogdan, A. R.; James, K. *Org. Lett.* **2011**, *13*, 4060–4063.
- (12) Schwartz, E.; Breitenkamp, K.; Fokin, V. V. *Macromolecules* **2011**, *44*, 4735–4741.
- (13) Juriček, M.; Stout, K.; Kouwer, P. H. J.; Rowan, A. E. *J. Porphyrins Phthalocyanines* **2011**, *15*, 905–907.
- (14) TBTA, the tris-triazole analogue to TTTA, but bearing benzyl chains instead of *tert*-butyl ones, costs more than 500 € per mmol (Sigma-Aldrich catalogue).
- (15)  $(N_C + N_O)/N_N \geq 3$  where  $N$  is the number of atoms, see: (a) Smith, P. A. S. *Open-Chain Nitrogen Compounds*, Vol. 2, Benjamin, New York, 1966, 211–246; (b) Boyer, J. H.; Moriarty, R.; de Darwent, B.; Smith, P. A. S. *Chem. Eng. News* **1964**, *42*, 6.
- (16) (a) Rodionov, V. O.; Presolski, S. I.; Gardinier, S.; Lim, Y.-H.; Finn, M. G. *J. Am. Chem. Soc.* **2007**, *129*, 12696–12704. (b) Rodionov, V. O.; Presolski, S. I.; Díaz Díaz, D.; Fokin, V. V.; Finn, M. G. *J. Am. Chem. Soc.* **2007**, *129*, 12705–12712.
- (17) For the elegant preparation of 5-iodotriazoles *via* the *in situ* electrophilic iodination of 5-H-triazoles, see: Brotherton, W. S.; Clark, R. J.; Zhu, L. *J. Org. Chem.* **2012**, *77*, 6443–6455.
- (18) (a) Díez-González, S.; Nolan, S. P. *Angew. Chem., Int. Ed.* **2008**, *47*, 8881–8884. (b) Díez-González, S.; Escudero-Adán, E. C.; Benet-Buchholz, J.; Stevens, E. D.; Slawin, A. M. Z.; Nolan, S. P. *Dalton Trans.* **2010**, *39*, 7595–7606. (c) Lal, S.; Díez-González, S. *J. Org. Chem.* **2011**, *76*, 2367–2373. (d) Lal, S.; McNally, J.; White, A. J. P.; Díez-González, S. *Organometallics* **2011**, *30*, 6225–6232.
- (19) (a) *N-Heterocyclic Carbenes: From Laboratory Curiosities to Efficient Synthetic Tools* (Ed: S. Díez-González), RSC, Cambridge, 2011. (b) Díez-González, S.; Marion, N.; Nolan, S. P. *Chem. Rev.* **2009**, *109*, 3612–3676. (c) *N-Heterocyclic Carbenes in Synthesis* (Ed: Nolan, S. P.), Wiley-VCH, Weinheim, 2006.
- (20) (a) Marion, N. 'NHC–Copper, Silver and Gold Complexes in Catalysis' in *N-Heterocyclic Carbenes: From Laboratory Curiosities to Efficient Synthetic Tools* (Ed: S. Díez-González), RSC, Cambridge, 2011. (b) Díez-González, S.; Nolan, S. P. *Aldrichimica Acta* **2008**, *41*, 43–51. For the most recent applications of copper–NHC complexes in cycloaddition reactions, see: (c) Gu, S.; Huang, J.; Liu, X.; Liu, H.; Zhou, Y.; Xu, W. *Inorg. Chem. Commun.* **2012**, *21*, 168–172. (d) Lazreg, F.; Slawin, A. M. Z.; Cazin, C. S. J. *Organometallics* **2012**, *31*, 7969–7975. (e) Hohloch, S.; Su, C.-Y.; Sarkar, B. *Eur. J. Inorg. Chem.* **2011**, 3067–3075. (f) Wang, W.; Wu, J.; Xia, C.; Li, F. *Green Chem.* **2011**, *13*, 3440–3445. (g) Nakamura, T.; Terashima, T.; Ogata, K.; Fukuzawa, S.-i. *Org. Lett.* **2011**, *13*, 620–623.
- (21) Clavier, H.; Nolan, S. P. *Chem. Commun.* **2010**, 46, 841–861.
- (22) Díez-González, S.; Scott, N. M.; Nolan, S. P. *Organometallics* **2006**, *25*, 2355–2358 See also reference 18a.
- (23) (a) Teyssot, M.-L.; Chevy, A.; Traïkia, M.; El-Ghozzi, M.; Avignant, D.; Gautier, A. *Chem.–Eur. J.* **2009**, *15*, 6322–6326. (b) Teyssot, M.-L.; Nauton, L.; Canet, J.-L.; Cisnetti, F.; Chevy, A.; Gautier, A. *Eur. J. Org. Chem.* **2010**, 3507–3515.
- (24) When to  $[\text{CuCl}(\text{IPr})]$  (0.5 mmol) in DCM (15 mL), phenanthroline (0.7 mmol) was added, the solution immediately turned red. Precipitation with petroleum ether yield a light red powder whose  $^1\text{H}$  NMR showed a mixture of starting material and a new compound which could be  $[\text{CuCl}(\text{IPr})(\text{phen})]$ . All attempts to separate both compounds failed. The lower conversion into a phen-adduct from  $[\text{CuCl}(\text{IPr})]$  when compared to  $[\text{CuCl}(\text{SImes})]$  is probably due to the higher steric hindrance of the IPr ligand. For the synthesis of a related Cu–IPr complex, see: Krylova, V. A.; Djurovich, P. I.; Whited, M. T.; Thompson, M. *Chem. Commun.* **2010**, 46, 6696–6698.
- (25) 78% and 61% conversion into triazole **1a** with 4 and 3 mol %  $[\text{CuCl}(\text{IPr})]$ , respectively.
- (26)  $[\text{CuCl}(\text{IPr})]$  is available from Sigma-Aldrich, Strem and TCI. For its synthesis, see: Jurkauskas, V.; Sadighi, J. P.; Buchwald, S. L. *Org. Lett.* **2003**, *5*, 2417–2420.
- (27) Campbell-Verduyn, L. S.; Mirfeizi, L.; Dierckx, R. A.; Elsinga, P. H.; Feringa, B. L. *Chem. Commun.* **2009**, 2139–2141 See also reference 18d.
- (28) (a) Pérez-Balderas, F.; Ortega-Muñoz, M.; Morales-Sanfrutos, J.; Hernández-Mateo, F.; Calvo-Flores, F. G.; Calvo-Asin, J. A.; Isac-García, J.; Santoyo-González, F. *Org. Lett.* **2003**, *5*, 1951–1954. (b) Gonda, Z.; Novak, Z. *Dalton Trans.* **2010**, 39, 726–729. (c) Wang, D.; Li, N.; Zhao, M.; Shi, W.; Ma, C.; Chen, B. *Green Chem.* **2010**, *12*, 2120–2123. (d) Wang, D.; Zhao, M.; Liu, X.; Chen, Y.; Li, N.; Chen, B. *Org. Biomol. Chem.* **2012**, *10*, 229–231. (e) Li, L.; Lopes, P. S.; Rosa, V.; Figueira, C. A.; Lemos, M. A. N. D. A.; Duarte, M. T.; Avilés, T.; Gomes, P. T. *Dalton Trans.* **2012**, 41, 5144–5154.
- (29) Apputkuttan, P.; Dehaen, W.; Fokin, V. V.; Van der Eycken, E. *Org. Lett.* **2004**, *6*, 4223–4225.
- (30) For a single example with a phosphite ligand, see: Nishizawa, Y. *Bull. Chem. Soc. Jpn.* **1961**, *34*, 1170–1178.
- (31) Scuster, I. I.; Roberts, J. D. *J. Org. Chem.* **1979**, *44*, 2658–2662.
- (32) Fife, D. J.; Moore, W. M.; Morse, K. W. *Inorg. Chem.* **1984**, *23*, 1684–1691.
- (33) Buckley, B. R.; Dann, S. E.; Heaney, H.; Stubbs, E. C. *Eur. J. Org. Chem.* **2011**, 770–776.
- (34) The dehalogenation of iodo(ethynylbenzene) had been observed in early tests, see Table 3.
- (35) (a) Cai, C.; Vasella, A. *Helv. Chim. Acta* **1995**, *78*, 2053–2064. Under our conditions no coupling of the halo- and terminal alkynes was observed, see: (b) Alami, M.; Ferri, F. *Tetrahedron Lett.* **1996**, *37*, 2763–2766.
- (36) Chai, J.-D.; Head-Gordon, M. *Phys. Chem. Chem. Phys.* **2008**, *10*, 6615–6620.
- (37) Weigend, F.; Ahlrichs, R. *Phys. Chem. Chem. Phys.* **2005**, *7*, 3297–3305.
- (38) Downing, J.; Murray-Rust, P.; Tonge, A. P.; Morgan, P.; Rzepa, H. S.; Cotterill, F.; Day, N.; Harvey, M. J. *J. Chem. Inf. Mod.* **2008**, *48*, 1571–1581.
- (39) (a) Scalmani, G.; Frisch, M. J. *J. Chem. Phys.* **2010**, *132*, 114110. (b) York, D. M.; Karplus, M. *J. Phys. Chem. A* **1999**, *103*, 11060–11079.
- (40) Carlqvist, P.; Eklund, R.; Brinck, T. *J. Org. Chem.* **2001**, *66*, 1193–1199.
- (41) Alvarez-Idaboy, J. R.; Reyes, L.; Cruz, J. *Org. Lett.* **2006**, *8*, 1763–1765.
- (42) For selected illustrative examples, see: (a) Lebel, H.; Janes, M. K.; Charette, A. B.; Nolan, S. P. *J. Am. Chem. Soc.* **2004**, *126*, 5046–5047. (b) Rasappan, R.; Hager, M.; Gissibi, A.; Reiser, O. *Org. Lett.* **2006**, *8*, 6099–6102. (c) Wang, D.; Cai, R.; Sharma, S.; Jirak, J.; Thummanapelli, S. K.; Akhmedov, N. G.; Zhang, H.; Liu, X.; Petersen, J. L.; Shi, X. *J. Am. Chem. Soc.* **2012**, *134*, 9012–9019 See also reference 18b.
- (43) Díez-González, S.; Nolan, S. P. *Coord. Chem. Rev.* **2007**, *251*, 874–883.
- (44) (a) Muetterties, E. L.; Alegranti, C. W. *J. Am. Chem. Soc.* **1970**, *92*, 4114–4115. (b) Lippard, S. J.; Mayerle, J. J. *Inorg. Chem.* **1972**, *11*, 753–759. (c) Fife, D. J.; Moore, W. M.; Morse, K. W. *Inorg. Chem.* **1984**, *23*, 1684–1691.
- (45) Reddy and co-workers reported the only ligandless catalytic system for this reaction: Reddy, K. R.; Venkateshwar, M.; Maheswari, C. U.; Kumar, P. S. *Tetrahedron Lett.* **2010**, *51*, 2170–2173 However, when we applied their reaction conditions (5 mol % CuI in DMSO at 80°C for 18 h) to our model reaction, only 8% conversion into triazole **1a** was obtained.
- (46) For the seminal report, see: (a) Staudinger, H.; Meyer, J. *Helv. Chim. Acta* **1919**, *2*, 635–646. For a review, see: (b) Gololobov, Y. G.; Kasukhin, L. F. *Tetrahedron* **1992**, *48*, 1353–1406.
- (47) See the Supporting Information for further details.
- (48) (a) Cristau, H. J.; Chiche, L.; Kadoura, J.; Torrelles, E. *Tetrahedron Lett.* **1988**, *29*, 3931–3934. (b) de la Fuente, G. F.; Huheey, J. E. *Phosphorus, Sulfur, and Silicon* **1993**, *78*, 23–36. (c) Molina, P.; López-Leonardo, C.; Llamas-Botía, J.; Foces-Foces, C.;

Fernández-Castaño, C. *Tetrahedron* **1996**, 52, 9629–9642. (d) Elson, K. E.; Jenkins, I. D.; Loughlin, W. A. *Aust. J. Chem.* **2004**, 57, 371–376.

(49) Himo, F.; Lovell, T.; Hilgraf, R.; Rostovtsev, V. V.; Noodleman, L.; Sharpless, K. B.; Fokin, V. V. *J. Am. Chem. Soc.* **2005**, 127, 210–216.

(50) For a related proposal with dinuclear copper(I) laderane complexes, see reference 9.

(51) Such  $\pi$ -activation is also believed to play an important role in the formation of copper-acetylide complexes, see: (a) Straub, B. F. *Chem. Commun.* **2007**, 3868–3870. (b) Ahlquist, M.; Fokin, V. V. *Organometallics* **2007**, 26, 4389–4391. See also: (c) Zhou, Y.; Lecourt, T.; Micouin, L. *Angew. Chem., Int. Ed.* **2010**, 49, 2607–2610.

(52) (a) Nolte, C.; Mayer, P.; Straub, B. F. *Angew. Chem., Int. Ed.* **2007**, 46, 2101–2103. For a recent report on a notable exception, see: Winn, J.; Pinczewska, A.; Goldup, S. M. *J. Am. Chem. Soc.* **2013**, 135, 13318–13321.

(53) Previous work by one of us already showed that copper-triazolides readily decompose, even in an argon-filled glovebox. See reference 18a for more details.

(54) Cantillo, D.; Ávalos, M.; Babiano, R.; Cintas, P.; Jiménez, J. L.; Palacios, J. C. *Org. Biomol. Chem.* **2011**, 9, 2952–2958.

(55) Cremer, D.; Krafka, E. *Acc. Chem. Res.* **2010**, 43, 591–601.

(56) (a) Cadiot, P.; Chodkiewicz, W. in *Chemistry of Acetylenes*, Viehe, H. G., ed, Marcel Dekker, New York, 1969; p 597. (b) Chodkiewicz, W. *Ann. Chim. Paris* **1957**, 2, 819–869.

(57) (a) Alami, M.; Ferri, F. *Tetrahedron Lett.* **1996**, 37, 2763–2766.

(b) Hosho, M.; Okimoto, M.; Nakamura, S.; Takahashi, S. *Synthesis* **2011**, 3839–3847.

(58) Worrell, B. T.; Malik, J. A.; Fokin, V. V. *Science* **2013**, 340, 457–460.

(59) Johnson, E. R.; Keinan, S.; Mori-Sánchez, P.; Contreras-García, J.; Cohen, A. J.; Yang, W. *J. Am. Chem. Soc.* **2010**, 132, 6498–6506.

(60) Armstrong, A.; Boto, R. A.; Dingwall, P.; Contreras-García, J.; Harvey, M. J.; Mason, N.; Rzepa, H. S. *Chem. Sci.* **2014**, 5, 2057–2071.